**Preprints of the 20th World Congress**
**The International Federation of Automatic Control**
**Toulouse, France, July 9-14, 2017**

# LPV model reduction methods for aeroelastic structures ⋆

**Gy. Lipták** * **T. Luspay** * **T. Péni** * **B. Takarics** * **B. Vanek** *

* *Institute for Computer science and Control (SZTAKI), H-1111 Budapest, Kende u. 13-17.*

**Abstract:** The aeroservoelastic modeling of flexible structures leads in general to large dimensional linear parameter varying (LPV) models. These models are intractable by the most analysis and control synthesis algorithms. Therefore, efficient model order reduction methods are needed. This paper investigates two approaches. Both are based on decoupling the large-scale model into smaller dynamical components, that are easier to reduce by balanced reduction techniques. While the first approach exploits the a-priori known, specific structure of the model, the second method algorithmically generates the low-level subsystems by performing a modal transformation and clustering the modes of similar dynamical behavior. The properties of the methods are analyzed via the reduction of the large-scale aeroelastic model of the BAH jet transport wing.

*Keywords:* Model reduction; Linear parameter-varying systems; Aerospace

## 1. INTRODUCTION

The future trends in aircraft design are oriented to build more economical aircrafts, i.e. to increase fuel efficiency and decrease the operating costs. To achieve these goals the decrease of the structural mass and the use of more flexible components is a possible way to go. Since in a more flexible aircraft the adverse aeroelastic effects (e.g. flutter) can occur even during normal operation, active control methods are needed to ensure the required flight envelope. To cope with this challenging task several research projects have been launched in the last few years, in both EU and US, e.g. (FLEXOP, 2015-2018) and (PAAW, 2014-2019).

In order to design a controller suppressing the aeroelastic effects, a suitable dynamic model is needed. Aeroservoelastic models can be constructed based on a subsystem approach: first a linear structural model is generated by finite element (FE) method, then it is interconnected with a linear aerodynamic model generated by Double Lattice Method (DLM) (Albano and Rodden, 1969). Due to the linear structure, the model is obtained in linear-parameter varying (LPV) form. In order to capture the relevant aeroelastic effects an accurate model is needed, which requires the use of a suitably dense structural grid and large number of lag states in the aerodynamic model. This results in a high-dimensional dynamical system (even with more than a hundred states), which is intractable by the most analysis and control synthesis algorithms based on semidefinite optimization and linear matrix inequalities (LMI) (Balas et al., 2015). This makes it necessary to develop an appropriate model order reduction method, which finds a lower dimensional representation for the same dynamical behavior.

This paper proposes two approaches for reducing the LPV model of aeroelastic structures. Both are based on the balanced reduction presented in (Wood, 1995). As the reduction algorithm involves a convex optimization problem with linear matrix inequalities (LMI) constraints, it has significant computational burdens. Therefore, to apply this method the initial model has to be decoupled into lower dimensional subsystems that can be independently reduced. The first is a generic procedure, which does not assume any special structural property of the initial model. It constructs an approximate modal decomposition and clusters the modes of similar dynamic behavior in order to generate independent subsystems that can be efficiently reduced. The algorithm is described in detail in (Gőzse et al., 2016; Luspay et al., 2016), where its main properties are also analyzed. The second method exploits the special structure of the aeroelastic model, which makes it possible to highly simplify the reduction procedure. The properties of the two approaches are analyzed and demonstrated on the reduction of the large scale LPV model of the BAH jet transport wing. This wing was first considered in (Bisplinghoff et al., 1955) and adapted as a demonstration problem in (Rodden et al., 1979). The aeroservoelastic model of the wing is available in the Nastran Aeroelasticity software package (Rodden and Johnson, 1994), where it is implemented as a benchmark example.

The paper is organized as follows. The introduction is followed by a short summary on balanced reduction. In Section 3 the aeroservoelastic modeling framework is outlined. Sections 5 and 4 are devoted to the two model reduction methods. The detailed comparison of the two approaches can be found in Section 6, where the numerical results obtained on the BAH wing model are analyzed. At the end of the paper the main results are collected and the most important conclusions are drawn.

## 2. PRELIMINARY RESULTS ON BALANCED MODEL REDUCTION

Consider a linear parameter varying (LPV) system in the usual state-space form as follows

$$\begin{aligned} \dot{x} &= A(\rho(t))x(t) + B(\rho(t))u(t) \\ y &= C(\rho(t))x(t) + D(\rho(t))u(t) \end{aligned} \tag{1}$$

where $x(t) \in \mathbb{R}^{n_x}, u(t) \in \mathbb{R}^{n_u}, y(t) \in \mathbb{R}^{n_y}$ are the state, input and output, respectively. In the paper we consider LPV models, where the scheduling variable $\rho(t)$ is scalar valued and both $\rho$ and $\dot{\rho}$ are defined over closed intervals $\Gamma$ and $\Omega$, respectively. We assume, on the other hand, that the dimension of $x$ is large, which makes the model intractable by most of the LPV analysis and synthesis

⋆ The research leading to these results is part of the FLEXOP project. This project has received funding from the European Unions Horizon 2020 research and innovation programme under grant agreement No 636307.

**Copyright by the International Federation of Automatic Control (IFAC)**

algorithms based on semidefinite optimization and linear matrix inequalities (LMI) (Balas et al., 2015). Therefore, it is necessary to reduce the model, i.e. to find a lower dimensional representation for the input/output behavior of (1).

Balanced reduction is one possible method to reduce a large-scale dynamical system. The approach is very efficient for LTI systems (Moore, 1981) and it has a theoretically sound extension to the parameter-varying case as well (Wood, 1995). The method is based on constructing a special, balancing state transformation that renders the observability and controllability Gramians equal and diagonal. Each diagonal entry, as being a generalization of the LTI Hankel singular values, provides quantitative measure for the observability and controllability of the associated state. Based on this information the less controllable and less observable states can be identified and eliminated (truncated or residualized).

The balancing transformation is constructed from the Gramians of (1). For an LTI system the Gramians are the unique, positive semidefinite solutions of the following two Lyapunov equations:

$$\begin{aligned} AX_c + X_cA^T + BB^T = 0 \\ A^TX_o + X_oA + C^TC = 0 \end{aligned} \tag{2}$$

Using $X_o$ and $X_c$ the Hankel singular values are computed as $\sigma_i = \sqrt{\lambda_i(X_oX_c)}$, $i = 1 \dots n_x$, while the balancing transformation is constructed by the algorithm described in detail in (Antoulas, 2005).

If in (2) the equality is replaced by negative semidefiniteness, the solutions $X_o \succeq 0$ and $X_c \succeq 0$ are the so called *generalized* Gramians, from which the generalized Hankel singular values can be computed. These are upper bounds for the Hankel singular values.

In LPV case only generalized Gramians exist, which could be parameter dependent. They can be computed by solving the following semidefinite optimization problem (Wood, 1995):

$$\min \operatorname{trace}(X_o(\rho)X_c(\rho)), \quad w.r.t. \quad X_o(\rho) \succeq 0, \quad X_c(\rho) \succeq 0$$

$$-\frac{d}{dt}X_c(\rho) + A(\rho)X_c(\rho) + X_c(\rho)A(\rho)^T + B(\rho)B(\rho)^T \preceq 0 \tag{3a}$$

$$\frac{d}{dt}X_o(\rho) + A(\rho)^TX_o(\rho) + X_o(\rho)A(\rho) + C(\rho)^TC(\rho) \preceq 0 \tag{3b}$$

The minimization of the singular values is necessary to get better controllability and observability measure for the states. In practice this nonlinear objective function is minimized by alternately solving (3) for $X_o(\rho)$ and $X_c(\rho)$. The infinite number of inequalities are relaxed to a finite set by evaluating (3b) and (3a) over a suitable dense grid $\underline{\rho} = \rho_1 < \rho_2 < \ldots < \rho_K = \overline{\rho}$. The details of the numerical algorithm as well as the construction of the parameter dependent balancing transformation can be found in (Wood, 1995). Since the transformation is parameter dependent, the transformed system and thus the reduced order model depends on $\dot{\rho}$ as well.

It is important to emphasize that the algorithm above works only if the system is stable. For marginally or unstable systems the method can still be applicable if a stable/unstable decomposition or a coprime factorization are performed on the initial model beforehand (Wood, 1995).

As algorithm (3) is based on semidefinite optimization, it is computationally demanding for large-scale systems. Since we intend to reduce aeroelastic models of more than a hundred state, (3) is not directly applicable. Therefore, the initial model is first decoupled into independent subsystems, which are then separately reduced. The first model reduction technique presented in Sec. 4 finds a possible decoupling by using a modal transformation and clustering, while the second (Sec. 5) follows the special model structure originated from the applied modeling framework.

## 3. AEROSERVOELASTIC MODELING

The aim of the current section is to present the basic concept and steps of aeroservoelastic modeling of the BAH wing. The BAH wing is a half wing with $b = 12.7\,m$ half wingspan, $\bar{c} = 4.1275\,m$ reference chord and $S = 52.42\,m^2$ wing area per side. It is fixed at the root and placed in an airflow of varying speed. The model is developed to describe the dynamic behavior of the wing around the flutter onset speed. The flutter onset speed is the lowest speed of the airflow at which structural damping is insufficient to compensate the increasing vibration caused by the aerodynamic forces and thus the structure goes unstable. The aim of the modeling presented in this section is to generate a precise dynamical model that can serve as a basis for a flutter suppression controller.

The aeroservoelastic model is developed based on a subsystem approach (Kier and Looye, 2009). The aerodynamics and the structural dynamics are developed separately and the interconnection forms the aeroservoelastic model (see Fig. 1).

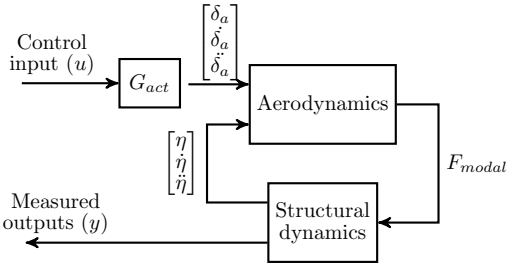


Fig. 1. Aeroelastic model

The structural model is obtained from a Finite Element (FE) approach (Rodden, 1967). A common element in such applications is the Euler-Bernoulli-beam with added torsional effects. The mass distribution of the wing is assumed to be replaced by a concentrated mass system based on physical considerations. The 10 structural grid points are placed forward and after along the concentrated masses as seen in Fig. 2 (Rodden and Johnson, 1994; Bisplinghoff et al., 1955). The 10 structural grid points have 1 degree of freedom, heaving in $z$ direction. Grid point 11 in Fig. 2 is fixed while grid point 12 represents the control surface deflection and can rotate along the $y$ axis. The structural model can be written as

$$M\ddot{\eta} + C\dot{\eta} + K\eta = F_{ext_{modal}} \tag{4}$$

where $M$, $C$ and $K$ are the modal mass, damping and stiffness matrices respectively and $F_{ext_{modal}}$ is the external excitation in modal coordinates. For the BAH wing model

$$F_{ext_{modal}} = F_{panel_{modal}} + F_{cs_{modal}} \tag{5}$$

where $F_{panel_{modal}}$ and $F_{cs_{modal}}$ are the external forces in modal coordinates resulting form the aerodynamic panel deformation and control surface deflection respectively. The elastic deformation of the $i^{th}$ structural grid point can be written in terms of modal coordinates $\eta$ and mode shapes $\Phi$ as $\delta_i = \sum_j^n \Phi_{ij}\eta_j$. In the present case the mode shapes relate the modal coordinates to the structural grid points heaving motion in $z$ direction. The mode shapes, mass and stiffness matrices with the rest of the parameter

values of the BAH wing can be found in (Rodden and Johnson, 1994). Note that the damping matrix of the BAH wing structural model is zero.

The unsteady aerodynamics is modeled with the subsonic DLM (Albano and Rodden, 1969). The model is divided into aerodynamic panels as shown in Fig. 2.

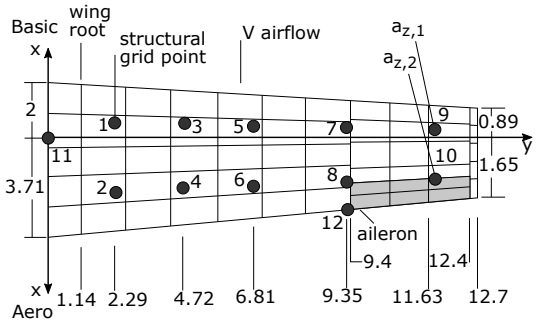


Fig. 2. BAH wing platform and aerodynamic strip idealization

A short summary of the generalized aerodynamic model for the aerodynamic panels is given based on (Rodden and Johnson, 1994; Kotikalpudi et al., 2015). The DLM results in the *AIC* (Aerodynamic Influence Coefficient) matrices that relate the normalwash vector $\bar{w}$ to the normalized pressure difference vector $\bar{p}$ about the panels as

$$\bar{p}_{panel} = [AIC_{panel}(\omega, V)]\,\bar{w} \tag{6}$$

where $\omega$ is the oscillating frequency and $V$ is the air speed. These two parameters are in general transformed into a single dimensionless parameter, the reduced frequency $k = \frac{\omega \bar{c}}{2V}$, where $\bar{c}$ is the reference chord length. In order to relate the modal displacements to the normalwash vector $\bar{w}$ and to transform the aerodynamic force to modal coordinates the so called generalized aerodynamic matrix (GAM) is defined as (see (Rodden and Johnson, 1994; Kotikalpudi et al., 2015) for more details)

$$Q_{panel}(k) = \Phi^T T_{as}^T S\,[AIC_{panel}(k)]\,(D_1 + ikD_2)\,T_{as}\Phi \tag{7}$$

where $D_1$ and $D_2$ are the differentiation matrices, $S$ is the integration matrix and $T_{as}$ is the interpolation matrix that projects the structural grid deformation on to the aerodynamic panels in form of their pitch and heave deformation (Kier and Looye, 2009). The GAM maps the modal deformation $\eta$ to the aerodynamic force distribution in modal coordinates $F_{panel_{modal}}$ as

$$F_{panel_{modal}} = \bar{q}\,[Q_{panel}(k)]\,\eta \tag{8}$$

where $\bar{q}$ is the free stream dynamic pressure. Since the GAM matrices are frequency dependent the resulting aerodynamic model is dynamic. Note that the GAM matrices are obtained only over a discrete reduced frequency grid. However, time domain aeroelastic simulations require a continuous model. There are several methods to obtain such models (Roger, 1977). Roger's rational function approximation (RFA) method (Roger, 1977) was applied applied for the BAH wing. The resulting aerodynamic model is obtained in the form

$$Q_{panel}(k) = Q_{panel_0} + Q_{panel_1} ik + Q_{panel_2}(ik)^2 + \sum_{l=1}^{n_p} Q_{panel_{l+2}} \frac{ik}{ik + b_l} \tag{9}$$

where $Q_{panel_0}$, $Q_{panel_1}$ and $Q_{panel_2}$ stand for the quasi-steady, velocity and acceleration terms of the aerodynamic model. The $Q_{panel_{l+2}}$ terms take the lag behavior of the aerodynamic model into account. The poles of the lag states are given by $b_l$. $n_p$ number of poles are selected for each modal coordinate a priori. This implies that the resulting aerodynamic model in general is of much higher dimension than the structural model. Note that RFA form of the GAM matrix given as (9) requires the modal coordinates $\eta$ and its the first and second time derivatives as input parameters.

In a similar fashion, the GAM matrices for the control surface deflection $\delta_a$ can be defined as

$$F_{cs_{modal}} = \bar{q}\,[Q_{cs}(k)]\,\delta_a \tag{10}$$

where $Q_{cs}(k)$ is the control surface GAM matrix. The actuator is defined based on (Brenner, 1996) as a $2^{nd}$ order linear model

$$G_{act}(s) = \frac{75^2}{s^2 + 2(0.59)(75)s + 75^2} \tag{11}$$

The RFA approximation of the control surface GAM matrix $Q_{cs}(k)$ requires the control surface deflection $\delta_a$ and its first and second time derivatives. Therefore, these signals are pulled out from the actuator dynamics.

Four signals are defined as the output of the BAH wing model. Two accelerometers are placed on the forward and aft structural grid points at the tip of the wing. Two angular rate sensors are placed at the same cross-section of the wing measuring the local pitch and roll rates respectively. Therefore, $y = [a_{z,1}\ \ a_{z,2}\ \ q\ \ p]^T$.

The structural dynamics of the BAH wing contains the first 10 structural modes and their time derivatives. This gives a 20 state model in the form of (4). The aerodynamic model is constructed by selecting $n_p = 8$ poles for each structural coordinate. Therefore, the aerodynamic model consists of 80 lag states with an additional 8 lag states for the aileron input. The aeroelastic model of the BAH wing including the actuator dynamics has therefore 110 states. The structural and the actuator models are linear while the aerodynamic model varies with the air speed. The resulting model is thus LPV and can be given in the form (1). The scheduling parameter $\rho$ is the airspeed defined in the interval $\Gamma := [121.92 \quad 640.08]$ m/s. The time derivative of the scheduling parameter is assumed to take values from the interval $\Omega = [-5, 5]$ m/s$^2$. The LPV model is given as a set of LTI systems obtained by evaluating the LPV model at 205 equidistant grid points defined over $\Gamma$. The flutter onset speed is at 343,11 m/s where the first bending and first torsion modes get coupled.

## 4. MODEL REDUCTION BASED ON MODAL DECOMPOSITION

This section describes the generic model reduction algorithm developed recently for LPV systems. It is assumed, that the dynamics are given in a standard grid-based representation, i.e.: a $K$ number of LTI models obtained by evaluating (1) at finite set of scheduling parameter values. The methodology is based on a consistent modal form of the underlying dynamics, which requires the $A(\rho)$ to be diagonalizable. The obtained LPV modal decomposition is then used for clustering system modes with dynamical similarity. Subsequently, smaller dimensional subsystems are reduced by using standard balancing transformations. Hereunder we give a brief overview of the algorithm, while the details can be found in (Gőzse et al., 2016; Luspay et al., 2016).

*LTI modal form.* Given a linear time invariant (LTI) system in state space form as $\dot{x} = Ax + Bu$. Assume $A$ is diagonalizable and let its eigenvalues and eigenvectors be denoted by $\lambda_i$ and $v_i$, respectively. Then $\hat{T} = [\Re(v_1)\ \ \Im(v_1)\ \ \ldots\ \ \Re(v_m)\ \ \Im(v_m)]$ defines a state transformation such that $\hat{A} := \hat{T}A\hat{T}^{-1}$ =block-diag$(\hat{A}_1, \ldots \hat{A}_m)$,

where each block corresponds to one dynamic mode, i.e.: $\hat{A}_i = \begin{bmatrix} \Re(\lambda_i) & \Im(\lambda_i) \\ -\Im(\lambda_i) & \Re(\lambda_i) \end{bmatrix}$ for complex conjugate eigenvalues and $\hat{A}_i = \lambda_i$ for real eigenvalues. The modal form is very powerful tool for model analysis and reduction, but its extension to linear parameter-varying systems is challenging, as discussed in the next sequel.

*LPV modal form.* Two main challenges are known in the literature regarding the construction of the modal form for LPV systems (Adegas et al., 2013). Firstly, one has to ensure the correct ordering of the modal blocks over the entire parameter domain. Secondly, the eigenspace (and hence the modal transformation) is parameter varying, where abrupt sign changes can appear, hindering the smooth interpolation of the transformed LTI systems. The following remedies are offered for these issues.

First of all, a scaling transformation is recommended for the grid-wise representation in order to improve the numerical conditioning of the eigenvalue and eigenvector computations. It is evident, that a constant $T$ transformation can be applied for every grid point, without affecting the IO behavior of the systems. After the scaling, the eigenvalue decomposition of the matrix sequence $A_k$, $k = 1, \ldots, K$ is carried out, resulting in a series of eigenvalues $\lambda_k$ and eigenvectors $v_k$ over the parameter domain. In order to assure the correct ordering of the eigenvalues, a metric is necessary to measure their distance. For this purpose, the pseudo-hyperbolic metric is adopted, which characterizes the dynamical similarity between two systems generated by the corresponding eigenvalues as poles (Gőzse et al., 2016). Computing pair-wise distances between eigenvalues of neighboring grid points, a minimal cost perfect matching problem can be formulated, for which effective numerical solutions are readily available. Consequently, eigenvalue trajectories are restored over the entire parameter domain and consistent order of the modal blocks are obtained. The details can be found in (Luspay et al., 2016).

The next step is the smoothing of the eigenspace, in order to facilitate smooth interpolation between each transformed LTI system. For this step, a complex Procrustes problem is formulated and solved for the corresponding sets of eigenvectors. Formally,

$$\overline{Q}_{k+1} = arg \min_{Q_{k+1}} \|V_k - V_{k+1} Q_{k+1}\|_F \,, \tag{12}$$

where $V_k$ and $V_{k+1}$ denote the eigenvectors at grid point $k$ and $k+1$ respectively. The $\overline{Q}_{k+1}$ solution of the Procrustes problem rotates neighboring eigenvectors close to each other, while preserving their eigen properties. Accordingly, abrupt sign changes and large variations in the eigenspace are eliminated and smoothed out.

Consequently, the parameter-varying modal transformation $\hat{T}(\rho)$ can be constructed on the analogy of the LTI case. Applying the state transformation ($\xi = \hat{T}(\rho)x$), the following LPV model is obtained:

$$\begin{aligned} \dot{\xi} &= \left( \hat{T}(\rho) A(\rho) \hat{T}^{-1}(\rho) + \frac{\partial \hat{T}(\rho)}{\partial \rho} \hat{T}^{-1}(\rho) \dot{\rho} \right) \xi + \hat{T}(\rho) B(\rho) u, \\ y &= C(\rho) \hat{T}^{-1}(\rho) \xi + D(\rho) u. \end{aligned} \tag{13}$$

Notice, that due to the parameter-dependence of the transformation $\hat{T}(\rho)$, the resulting system depends also on $\dot{\rho}$ in (13). At the same time, this dependence generally can be neglected in most of the cases, because the Procrustes smoothing minimizes the $\frac{\partial \hat{T}(\rho)}{\partial \rho}$ gradient of the modal transformation. Consequently, a quasi-modal form is obtained, which is used for model order reduction.

*Hierarchical clustering.* The parameter-varying quasi-modal form is very attractive and useful, since various information can be easily extracted from this representation. Firstly, a stable-unstable decomposition can be performed, where unstable modes can be separated (and exactly preserved) from the stable parts. Secondly, modes which are outside of the frequency range of interest can be removed as well. This is a rather useful aspect of the methodology in the context of reduced-order controller design. Hence, only stable modes within the frequency range are kept and reduced.

In order to obtain a numerically solvable problem for model reduction, the system is broken apart for several subsystems. The key idea is to create small dimensional subsystems representing similar dynamical behavior of the full-order model. Accordingly, system modes are grouped together by using hierarchical clustering (Hastie et al., 2009). Dynamic similarity of parameter-varying modes are measured through the extension of the pseudo-hyperbolic metric, then, the successive evaluation of the distances are performed. In each step those clusters are merged together for which the smallest pseudo-hyperbolic distance is obtained, repeated until a single cluster is obtained. The merging is usually illustrated on a tree diagram (called dendrogram), where the user can determine the level of similarity for the final cluster structure (Hastie et al., 2009). Accordingly, the system can be decomposed into several smaller dimensional subsystems, each collecting similar dynamical behaviors together.

*Balanced reduction.* The balanced reduction of each subsystem is performed next. Parameter-varying observability and controllability Gramians are computed first, followed by the corresponding balancing transformations. The parameter-varying singular values provide information about the number of states that can be eliminated without effecting the corresponding dynamical behavior. Therefore, each subsystem is reduced individually. It is then possible to merge the reduced subsystems into a single model, where a second balanced reduction can be performed. The idea behind this step is twofold. First, the dimension of the corresponding system does not hinder the numerical computations any more. Second, the additional balancing can reveal further information on eliminating states irrelevant of the overall input-output behavior. Upon performing the second reduction, unstable modes can be reinstated to conclude the parameter-varying reduction.

## 5. STRUCTURED MODEL REDUCTION

The model reduction method presented in this section starts from the model structure in Fig 1 and considers the subsystems independently. The actuator model is typically a simple LTI system, so it cannot be further reduced. The structural dynamics are also LTI, though it is marginally stable if - as in the BAH wing model - the damping matrix is 0. This makes it necessary to use model reduction algorithms extended to unstable/marginally stable systems. The only parameter-varying block in Fig 1 is the aerodynamics. In the sequel we focus on the reduction of this block. It will be shown that the special structure of its parameter dependence makes it possible to apply balanced reduction without solving the semidefinite optimization (3).

Consider the aerodynamic model in LPV form as follows

$$\begin{aligned} \dot{x}_{ae} &= \underbrace{\rho A_1}_{A_{ae}(\rho)} x_{ae} + \underbrace{B_0}_{B_{ae}(\rho)} u_{ae} \\ y_{ae} &= \underbrace{\rho^2 C_2}_{C_{ae}(\rho)} x_{ae} + \underbrace{(D_0 + \rho D_1 + \rho^2 D_2)}_{D_{ae}(\rho)} u_{ae} \end{aligned} \tag{14}$$

where the matrices $A_1, B_0, C_2, D_i$ are all constant. The vector $x_{ae} \in \mathbb{R}^{n_{ae}}$ is the state vector of the aerodynamics. The input vector $u_{ae}$ contains the modal coordinates, the control input and their first and second derivatives. The output vector $y_{ae}$ collects the generalized forces which are in the modal coordinate system.

To construct the Gramians, consider first inequality (3a). By substituting the LPV model (14) it takes the form

$$\rho A_1 X_c(\rho) + X_c(\rho)(\rho A_1)^T + B_0 B_0^T - \dot{X}_c(\rho) \preceq 0 \quad (15)$$

Let $X_c(\rho) = \frac{1}{\rho}\overline{X}_c$ and thus $\dot{X}_c(\rho) = -\frac{\dot{\rho}}{\rho^2}\overline{X}_c$, where $\overline{X}_c$ is a constant matrix. Then the LMI above can be written as

$$(A_1 + \frac{\dot{\rho}}{2\rho^2} I)\overline{X}_c + \overline{X}_c(A_1 + \frac{\dot{\rho}}{2\rho^2} I)^T + B_0 B_0^T \preceq 0 \quad (16)$$

Since both $\dot{\rho}$ and $\rho$ are bounded, the term $\frac{\dot{\rho}}{2\rho^2}$ has a maximum over $\Gamma \times \Omega$. Let this maximum be denoted by $\alpha$. We can now consider the following Lyapunov *equality* instead of the inequality above:

$$(A_1 + \alpha I)\overline{X}_c + \overline{X}_c(A_1 + \alpha I)^T + B_0 B_0^T = 0 \quad (17)$$

Note that, this equation has a unique positive semidefinite solution $\overline{X}_c$ if $(A_1 + \alpha I)$ is a Hurwitz matrix. Furthermore, if $\overline{X}_c \succeq 0$ is a solution then $X_c(\rho) = \frac{1}{\rho}\overline{X}_c$ satisfies inequality (15) for all $\rho \in \Gamma$ and $\dot{\rho} \in \Omega$. Thus $X_c(\rho)$ is a controllability Gramian for (14) and it has been constructed by solving only a set of linear equations instead of performing the computationally demanding semidefinite optimization (3).

As for the observability Gramian $X_o(\rho)$, a similar procedure can be applied. For this we start from the LMI

$$(\rho A_1)^T X_o(\rho) + X_o(\rho)\rho A_1 + (\rho^2 C_2)^T \rho^2 C_2 + \dot{X}_o(\rho) \preceq 0 \quad (18)$$

If $X_o(\rho) = \rho^3 \overline{X}_o$ and thus $\dot{X}_o(\rho) = 3\rho^2\dot{\rho}\overline{X}_o$ then the LMI above takes the following simpler form:

$$(A_1 + \frac{3\dot{\rho}}{2\rho^2} I)^T \overline{X}_o + \overline{X}_o(A_1 + \frac{3\dot{\rho}}{2\rho^2} I) + C_2^T C_2 \preceq 0 \quad (19)$$

Let $\beta = \max \frac{3\dot{\rho}}{2\rho^2}$ and consider the Lyapunov equality

$$(A_1 + \beta I)^T \overline{X}_o + \overline{X}_o(A_1 + \beta I) + C_2^T C_2 = 0 \quad (20)$$

Again, this equation has a unique positive definite solution $\overline{X}_o$ if $(A_1 + \beta I)$ is Hurwitz and if $\overline{X}_o \succeq 0$ solves (17) then $X_o(\rho) = \rho^3 \overline{X}_o$ satisfies (18).

From $X_o(\rho)$ and $X_c(\rho)$ we can now construct the balancing state transformation $T(\rho)$. Instead of performing the standard procedure described in (Wood, 1995), we use now a different approach resulting in a *parameter independent* state transformation $\overline{T}$ that also transforms the system in a form in which the less observable and less controllable states can be identified but as it being constant, the reduced order model will not depend on $\dot{\rho}$.

For this, consider the generalized Hankel singular values of system (14)

$$\sigma_i(\rho) = \sqrt{\lambda_i(X_c(\rho)X_o(\rho))} = \rho\sqrt{\lambda_i(\overline{X}_c\overline{X}_o)} = \rho\overline{\sigma}_i \quad (21)$$

Since the positive valued scheduling parameter acts only as a scaling, the information on the observability and the controllability of the states is carried by the constant $\overline{\sigma}_i$ values . Therefore, we can choose $\overline{T}$ to be the constant balancing transformation computed from $\overline{X}_c$ and $\overline{X}_o$. Then, by definition $\overline{T}^{-1}\overline{X}_c\overline{T}^{-T} = \overline{T}^T\overline{X}_o\overline{T} = \mathrm{diag}(\overline{\sigma}_1, \ldots, \overline{\sigma}_{n_{ae}})$. Defining $\tilde{x}_{ae} = \overline{T}x_{ae}$ the Gramians of the transformed LPV system can be obtained as follows:

$$\tilde{X}_c(\rho) = \overline{T}^{-1} X_c(\rho) \overline{T}^{-T} = \frac{1}{\rho}\mathrm{diag}(\overline{\sigma}_1, \ldots, \overline{\sigma}_{n_{ae}}) \quad (22)$$

$$\tilde{X}_o(\rho) = \overline{T}^T X_o(\rho)\overline{T} = \rho^3 \mathrm{diag}(\overline{\sigma}_1, \ldots, \overline{\sigma}_{n_{ae}}), \quad (23)$$

Consequently, the states of $\tilde{x}_{ae}$ associated with small $\overline{\sigma}_i$ value are less controllable and less observable, so they can be eliminated from the model. It can also be checked that either truncation or residualization is applied the simple structure of the parameter dependence is preserved in the reduced order model, i.e. $A_{ae,r}(\rho) = \rho A_{1,r}$, $C_{ae,r}(\rho) = \rho^2 C_{2,r}$, $D_{ae,r}(\rho) = D_{0,r} + \rho D_{1,r} + \rho^2 D_{2,r}$.

## 6. NUMERICAL RESULTS - REDUCTION OF THE BAH WING MODEL

In this section the detailed comparison of the two methods is presented through the numerical results obtained for the BAH wing model.

*Model decompositions* Although, the two methodologies represent two different approaches, it is very interesting and useful to take a closer look on the decompositions in each frameworks. The structured model reduction exploits the underlying interconnection as depicted in Fig. 1. Analyzing the IO behaviors, it is found that neither the LTI structural dynamics, nor the actuator dynamics can be further reduced by using standard techniques. That is, only the 88 dimensional aerodynamics block is subject of the model reduction, as discussed in Section 5. On the other hand, the generic LPV model reduction methodology in Section 4 does not incorporate explicitly the specific structure of the model. Instead, the hierarchical clustering is applied to exploit the dynamical structure of the system. For this, the approximate modal decomposition has to be constructed first. By performing time-domain Monte Carlo simulations it can be checked that the $\dot{\rho}$-dependent, coupling terms in (13) can be neglected without causing significant change in the IO behavior. Therefore, the modal system depends only on $\rho$. Continuing the process by removing the unstable modes, the 106 dimensional stable part is subdivided into 13 clusters. Nine of these clusters are 2 dimensional, containing dynamics of a single complex-conjugate mode. Obviously, these are non-reducible blocks. Therefore, only the remaining 4 clusters can be reduced, with the following dimensions: 22,21,24 and 21; altogether 88 states are subject to the balancing model reduction described in Section 4. The corresponding dynamics are clearly related to the aerodynamics block, where due to the feedback configuration complex modes appear. This similarity verifies the proposed hierarchical clustering approach of the modal-based LPV model reduction algorithm.

*Model reduction* The special parameter dependence of the aerodynamics block is utilized in the structured reduction algorithm. Consequently the problem is boiled down to a parameter-independent one, as discussed in Section 5. This approximation does not suffer from the curse of dimensionality (in contrast to LMI methods), hence it is possible to compute the 88 dimensional Gramians of the corresponding Lyapunov equalities. Based on the Hankel singular values 76 states can be neglected, resulting in a 34 dimensional reduced model. At the same time, further reduction of the aerodynamic block is still possible due to the feedback configuration. Hence an additional 6 states are removed, obtaining a 28 dimensional approximation of the original dynamics. Under the generic framework, LPV balancing methods are used for reducing the smaller dimensional clusters. For each subsystem a parameter-independent controllability and observability Gramians is searched and computed by solving the iterative optimization over LMI constraints (Wood, 1995). The corresponding singular values imply 6, 12, 12 and 10 significant states

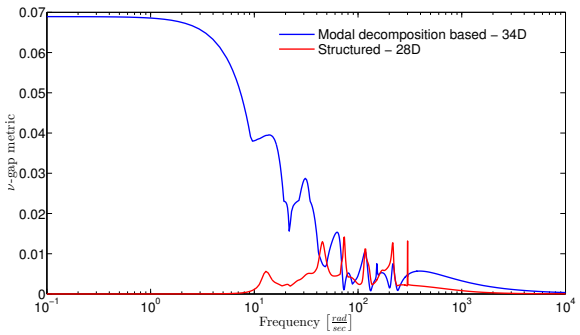


Fig. 3. Frequency distribution of the $\nu$-gap

for the respective subsystems. Accordingly, the 88 dimensional LPV system is reduced to 40 dimensional. Nevertheless, this state dimension can also be further reduced, after joining the reduced subsystems together. A second balanced reduction is then applied for the 40 dimensional system, where an additional 24 states are eliminated successfully. This step takes into consideration the relative contributions of the subsystems in the overall IO behavior of the model. Hence, the final LPV approximation is 34 dimensional.

*Numerical aspects* As discussed above, the two approaches use different numerical solutions. The structured methodology relies on Lyapunov equalities, which is certainly a much more well conditioned problem than the inequality based solution of the generic LPV reduction. The number of decision variables is $3916 \times 2$ for the corresponding Lyapunov equalities, which can be solved in $1sec$ using the available SLICOT's solver SB03MD under MATLAB. For the modal-decomposition based approach the decision variables are: $253 \times 2$, $231 \times 2$, $300 \times 2$ and $231 \times 2$ for the respective $22, 21, 24$ and $21$ dimensional clusters. The corresponding LMIs are solved in an iterative manner, where each step takes approximately $60secs$ by using the MOSEK semidefinite solver under MATLAB.

*Comparison* The model reduction is often motivated by the computational limitations of the controller design, hence the $\nu$-gap metric is chosen to evaluate the goodness of the reduced-order models (Vinnicombe, 1993). The $\nu$-gap between the full- and reduced-order models characterizes the stability margin of the controllers working with the former and designed for the latter. The $\delta_\nu(\rho, \omega)$ function is constructed by computing point-wise $\nu$-gap over a two-dimensional grid of the scheduling parameter $\rho$ and frequency range $\omega$. Moreover, Figure 3 shows the frequency distribution of $\delta_\nu(\rho, \omega)$, i.e.: $\max_\rho \delta_\nu(\rho, \omega)$. It can be seen that the two models approximate the full-order system equally good on middle and high frequency ranges. However, the balanced truncation of the generic LPV reduction method leads to higher $\nu$-gap values in the low frequency range. Nonetheless, the results are still promising.

## 7. CONCLUSION

In the paper two methods have been proposed for reducing large scale aeroelastic models. To demonstrate the applicability of the algorithms to reveal their most important properties the 110 dimensional model of the BAH transport jet wing has been reduced. The presented approaches will be used to generate a numerically tractable LPV model for the FLEXOP demonstrator aircraft, which will be flight tested in 2018.

## REFERENCES

Adegas, F., Sonderby, I., Hansen, M.H., and Stoustrup, J. (2013). Reduced-order LPV model of flexible wind turbines from high fidelity aeroelastic codes. In *IEEE Conference on Control Applications*, 424–429.

Albano, E. and Rodden, W. (1969). A doublet-lattice method for calculating lift distributions on oscillating surfaces in subsonic flows. *Journal of Aircraft*, 7(2), 279–285.

Antoulas, A.C. (2005). *Approximation of Large-Scale Dynamical Systems*. Advances in Design and Control. SIAM.

Balas, G., Hjartarson, A., Packard, A., and Seiler, P. (2015). *LPVTools: A Toolbox for Modeling, Analysis, and Synthesis of Parameter Varying Control Systems*. Musyn, Inc. URL `http://www.aem.umn.edu/~SeilerControl/software.shtml`.

Bisplinghoff, R.L., Ashley, H., and Halfman, R.L. (1955). *Aeroelasticity*. Addison-Wesley Publishing Company.

Brenner, M.J. (1996). Aeroservoelastic Modeling and Validation of a Thrust-Vectoring F/A-18 Aircraft. Technical report, NASA, Dryden Flight Research Center.

FLEXOP (2015-2018). Flutter Free FLight Envelope eXpansion for ecOnomical Performance improvement (FLEXOP). Project of the European Union, Project ID: 636307.

Gőzse, I., Luspay, T., Péni, T., Szabó, Z., and Vanek, B. (2016). Model Order Reduction of LPV Systems Based on Parameter Varying Modal Decomposition. In *IEEE Conference on Decision and Control*.

Hastie, T., Tibshirani, R., and Friedman, J. (2009). *The Elements of Statistical Learning*. Data Mining, Inference, and Prediction. Springer.

Kier, T.M. and Looye, G.H.N. (2009). Unifying manoeuvre and gust loads analysis models. In *International Forum on Aeroelasticity and Structural Dynamics (IFASD)*, 1–20.

Kotikalpudi, A., Pfifer, H., and Balas, G.J. (2015). Unsteady Aerodynamics Modeling for a Flexible Unmanned Air Vehicle. In *AIAA Atmospheric Flight Mechanics Conference*.

Luspay, T., Péni, T., Gőzse, I., Szabó, Z., and Vanek, B. (2016). Model reduction for LPV systems based on approximate modal decomposition. *Submitted to Int. J. of. Robust Nonlin. Control, but can be accessed in arXiv under reference number arXiv:1609.06948*.

Moore, B.C. (1981). Principle Component Aanalysis in Linear Systems: Controllability, Observability, and Model Reduction. *IEEE Transactions on Automatic Control*, 26(1), 17–32.

PAAW (2014-2019). Performance Adaptive Aeroelastic Wing Program. Supported by NASA NRA "Lightweight Adaptive Aeroelastic Wing for Enhanced Perfromace Across the Flight Envelope".

Rodden, W.P. (1967). A method for deriving structural influence coefficients from ground vibration tests. *AIAA Journal*, 5(5), 991–1000.

Rodden, W.P., Harder, R.L., and Bellinger, E.D. (1979). Aeroelastic Addition to NASTRAN. Technical report, NASA Contractor Report 3094.

Rodden, W.P. and Johnson, E. (1994). MSC/NASTRAN Aeroelastic Analysis: User's Guide, Version 68.

Roger, K.L. (1977). Airplane Math Modeling Methods for Active Control Design. Structural Aspects of Active Controls. In *Structural Aspects of Active Controls, AGARD-CP-228*, 4–11.

Vinnicombe, G. (1993). *Measuring Robustness of Feedback Systems*. Ph.D. thesis, Department of Engineering, University of Cambridge.

Wood, G.D. (1995). *Control of Parameter-Dependent Mechanical Systems*. Ph.D. thesis, University of Cambridge.